The EMBO Journal vol.7 no.11 pp.3571 - 3576, 1988

A model for the spatial arrangement of the proteins in the large subunit of the *Escherichia coli* ribosome

Jan Walleczek, Dierk Schüler, Marina Stöffler-Meilicke[2], Richard Brimacombe* and Georg Stöffler[1]

Max-Planck-Institut für Molekulare Genetik, Abteilung Wittmann, Ihnestrasse 73, D-1000 Berlin 33 (Dahlem), FRG and [1]Institut für Mikrobiologie, Medizinische Fakultät der Universität Innsbruck, Fritz-Pregl-Str.3, A-6020 Innsbruck, Austria

[2]Present address: Institut für Mikrobiologie, Medizinische Fakultät der Universität Innsbruck, Fritz-Pregl-Str.3, A-6020 Innsbruck, Austria

*Reprint requests

Communicated by H.Wittman

A three-dimensional model for the arrangement of 29 of the 33 proteins from the *Escherichia coli* large ribosomal subunit has been generated by interactive computer graphics. The topographical information that served as input in the model building process was obtained by combining the immunoelectron microscopically determined network of epitope-epitope distances on the surface of the large ribosomal subunit with *in situ* protein-protein cross-linking data. These two independent sets of data were shown to be compatible by geometric analysis, thus allowing the construction of an inherently consistent model. The model shows (i) that the lower third of the large subunit is protein-poor, (ii) that proteins known to be functionally involved in peptide bond formation and translocation are clustered in two separate regions, (iii) that proteins functionally interdependent during the self-assembly of the large subunit are close neighbours in the mature subunit and (iv) that proteins forming the early assembly nucleus are grouped together in a distinct region at the 'back' of the subunit.

Key words: computer graphics/immunoelectron microscopy/protein-protein crosslinking/protein topography/ribosome structure

Introduction

Polypeptide formation from aminoacyl-tRNA under the control of mRNA occurs on ribosomes in all organisms. One fundamental prerequisite for understanding the mechanisms underlying this central function is a detailed knowledge of the structure of the ribosome at the amino acid/nucleotide level. However, a determination of the structure of the ribosome at this resolution will not be available for some time, and until then, models at lower levels of resolution have to be used in trying to correlate ribosomal structure and function.

Recently, several such models have been presented for the small 30S ribosomal subunit of *Escherichia coli*, based on data from immunoelectron microscopy (IEM) (Stöffler-Meilicke and Stöffler, 1987), neutron scattering (Capel *et al.*, 1987) and RNA-RNA and RNA-protein cross-linking (Brimacombe *et al.*, 1988). In contrast, the models for the spatial arrangement of the proteins within the large 50S ribosomal subunit that so far have been proposed (Stöffler and Stöffler-Meilicke, 1986; Nowotny *et al.*, 1986) are far less complete, and do not yet give a consistent model for the protein topography of the large subunit. Therefore, using interactive computer graphics, we have developed a strategy for constructing topographical models of complex structures such as the ribosome, which allows the incorporation of geometric information from any experiment yielding distance data between the individual components of the structure under investigation. Thus, even incomplete and different sets of data (e.g. distance data derived from IEM, neutron scattering, chemical cross-linking, fluorescence energy transfer measurements etc.) can in principle be used to generate three-dimensional models.

The outcome of the work described in this paper is a model of the protein topography for 29 of the 33 different ribosomal proteins of the 50S subunit. The model is consistent with the relevant topographical data from other independent studies that were not used in the generation of the model. One feature of the model is that the different proteins are not distributed evenly throughout the subunit, but that the region in the lower third of the subunit appears to be protein-poor. Furthermore, a number of structure-function correlations are revealed by comparing the model with data from functional studies. First, the proteins known to be functionally involved in peptide bond formation (Auron and Fahnestock, 1981; Schulze and Nierhaus, 1982) are grouped together in a region close to the 'core' of the subunit, and the proteins functionally involved in the GTPase activity (Möller and Maassen, 1986) are grouped together in the 'L7/12-stalk' domain. Secondly, proteins which interact during the self-assembly of the 50S subunit from its RNA and protein constituents (Herold and Nierhaus, 1987) are located close to each other in the mature subunit. Thirdly, proteins initiating the assembly of the 50S subunit (Herold and Nierhaus, 1987) are neighbours at the 'back' of the particle, suggesting that this region of the subunit serves as the assembly initiation region.

Data used in the generation of the model

It is clear that the reliability of any spatial model depends primarily on the quality of the data used in its construction. For this reason, in this work we have exclusively used data derived from sources that are of proven reliability. The primary data set used to generate the model was the relative spatial arrangement of epitopes of different ribosomal proteins on the surface of the 50S ribosomal subunit, as determined by IEM (Stöffler and Stöffler-Meilicke, 1986; Hackl *et al.*, 1988; W.Hackl and M.Stöffler-Meilicke, in preparation). We are confident that these data for the 50S ribosomal subunit are reliable, since for all proteins used in the model building process stringent specificity controls have been performed (Stöffler and Stöffler-Meilicke, 1985). Furthermore, a comparison of the most recent models of the 30S ribosomal subunit derived from IEM (Stöffler-

©IRL Press Limited, Oxford, England

Table I. Protein–protein cross-links compared with IEM data

Protein–protein cross-link	Reference	Length of cross-linker	A	Epitope–epitope distance
L1–L33	a	11	75	NA
L2–L9	b	5	80	45
L3–L13	b	5	77	NA
L3–L19	b	4	73	NA
L6–L19	a	11	78	50
L7/12–L10	a	11	114	20
L7/12–L11	a	11	112	55
L9–L28	b	5	66	NA
L10–L11	b	4	72	55
L13–L20	b	5	71	NA
L13–L21	b	4	68	NA
L14–L19	b	4	68	30
L14–L32	c	12	69	NA
L16–L27	b	5	66	NA
L17–L30	d	14	72	NA
L17–L32	b	5	62	NA
L18–L22	a	11	73	NA
L19–L25	a	11	72	90
L20–L21	b	5	67	NA
L22–L32	d	14	70	NA
L23–L29	b	5	61	55
L23–L34	d	14	68	NA
L27–L33	a	11	64	NA

The table lists the protein–protein cross-links used to generate the model, the maximum length of the cross-linking reagent in each case, the maximum distance A between points on the respective protein surfaces (see text for calculation of this parameter), and the corresponding epitope–epitope distances (where these are available). Proteins that have also been mapped by IEM on the surface of the 50S ribosomal subunit are underlined. The epitope–epitope distances were taken from the IEM-model (Stöffler and Stöffler-Meilicke, 1986; Hackl *et al.*, 1988; W.Hackl and M.Stöffler-Meilicke, in preparation). NA means not available. The cross-links were identified by immunoblotting (Stöffler *et al.*, 1988), except for the complex L14–L32 which was identified by sequencing the N termini of the crosslinked proteins. All values are given in Angström units. The references are: (a) B.Redl, J.Walleczek, M.Stöffler-Meilicke and G.Stöffler, in preparation; (b) J.Walleczek, T.Martin, B.Redl, M.Stöffler-Meilicke and G.Stöffler, in preparation; (c) T.Pohl and B.Wittmann-Liebold, in preparation; (d) J.Walleczek, B.Redl, M.Stöffler-Meilicke and G.Stöffler, in preparation.

Meilicke and Stöffler, 1987), from neutron scattering (Capel *et al.*, 1987) and from a model showing the optimized three-dimensional fit between ribosomal proteins and the 16S rRNA (Schüler and Brimacombe, 1988) shows an excellent agreement with regard to the proposed three-dimensional positions of the individual proteins. It can therefore be concluded that the IEM-method as applied yields reliable topographical data.

A second set of data comes from recent protein–protein cross-linking studies, using specific immunoreactions in order to guarantee an unambiguous identification of the proteins in the cross-linked protein complexes (Stöffler *et al.*, 1988). The superiority of this approach over other identification methods is discussed elsewhere (J.Walleczek, B.Redl, M.Stöffler-Meilicke and G.Stöffler, in preparation).

Thus, a total of 171 epitope–epitope distances between 19 different proteins on the surface of the 50S ribosomal subunit taken from the IEM-model (Stöffler and Stöffler-Meilicke, 1986; Hackl *et al.*, 1988; W.Hackl and M.Stöffler-Meilicke, in preparation), and 23 distances between reactive groups of 26 different ribosomal proteins as determined by chemical cross-linking (see Table I) were used to generate the model. However, before these two sets of independent data could be incorporated into a single coherent model, it was first necessary to demonstrate their mutual compatibility.

Table II. Positions of the ribosomal proteins in the model

Protein	Radius	Position		
		x	y	z
L1	19.5	15	18	17
L2	20.8	60	−27	34
L3	18.9	109	−52	36
L4	18.9	45	−33	75
L5	18.3	89	32	8
L6	17.9	152	−20	1
L7/12	[a]	190	47	3
L9	16.8	28	−16	11
L10	17.5	164	1	24
L11	16.5	182	−8	1
L13	16.9	120	−42	68
L14	16.0	117	−19	18
L15	16.6	59	11	43
L16	16.7	95	−24	42
L17	16.3	146	−65	68
L18	15.7	113	51	16
L19	15.8	126	−37	3
L20	16.0	146	−13	72
L21	15.2	117	−14	61
L22	15.5	124	3	39
L23	15.0	59	−93	66
L25	14.8	126	24	17
L27	14.0	84	0	37
L28	13.9	27	−24	40
L29	13.0	42	−63	65
L30	12.5	119	−67	62
L32	12.4	136	−32	50
L33	12.4	54	2	18
L34	11.8	73	−72	46

The positions of the proteins are given in terms of the Cartesian coordinates in the model of the geometric centres of the protein spheres representing the individual proteins. The radii of the proteins and the coordinates are given in Angström units. The radii of the proteins were determined as described in the text.
[a]Proteins L7/12 are present in four copies per 50S ribosomal subunit and are represented in the model as an ellipsoid with half-axes of 35 and 17 Å, respectively.

Comparison of the IEM and cross-linking data

In order to determine whether or not the data from IEM and protein–protein crosslinking are compatible, the two sets of data were compared as follows. The largest possible distance (A) between two points on the surface of two proteins which are either connected directly by a cross-link, or cross-linked via one or more intermediate proteins, is given by the relation

$$A = (2r_1 + 2r_2 + \ldots) + (a_1 + a_2 + \ldots),$$

where r_1, r_2, etc. represent the radii of the proteins in the cross-linked complex(es) and a_1, a_2, etc. represent the maximum lengths of the cross-linking reagents used. The topographical data for a protein pair from IEM and

protein−protein cross-linking are compatible if A is larger than or equal to the epitope−epitope distance between the two proteins of the pair, as determined by IEM. The results of this comparison can be seen in Table I, the appropriate values for r being taken from Table II: seven of the eight protein pairs which could be tested in this way are fully compatible, and only the protein pair L19−L25 shows a value of A that is less than the epitope−epitope distance. However, even in this case the deviation is only 9 Å for each member of the protein pair and is well within the limits of accuracy of the IEM-determination. Table I thus shows that, in those cases where a comparison is possible, the IEM and cross-linking data are indeed compatible.

Generation of the model

The model was generated in two consecutive steps: (i) The coordinates of the surface shape and the protein epitopes on the surface were measured from the IEM-model of the 50S ribosomal subunit (Meisenberger *et al.*, 1984; Stöffler and Stöffler-Meilicke, 1986; Hackl *et al.*, 1988; W.Hackl and M.Stöffler-Meilicke, in preparation) and were fed into the computer graphics system. (ii) The three-dimensional positions of the individual ribosomal proteins were derived by interactively incorporating into the model the geometric information from the recent protein−protein cross-linking results (see Table I).

In the first step the shape of the model of the 50S ribosomal subunit from electron microscopic studies (Meisenberger *et al.*, 1984; Stöffler and Stöffler-Meilicke, 1986) was reconstructed by feeding the data for the surface shape into the computer graphics system. This particular shape was the one used to interpret the protein positions from the IEM data. The spatial dimensions of the resulting object were then adjusted by incorporating the most recently estimated values for the dimensions in Cartesian x-, y- and z-axes obtained from image reconstruction analysis of electron micrographs of the 50S ribosomal subunits, namely 215 Å, 245 Å and 140 Å, respectively (Radermacher *et al.*, 1987). Next, the relative positions of 19 epitopes of the ribosomal proteins that have been mapped by IEM (Stöffler and Stöffler-Meilicke, 1986; Hackl *et al.*, 1988; W.Hackl and M.Stöffler-Meilicke, in preparation) on the surface of the 50S subunit were constructed from 171 distance pairs between these epitopes. Each epitope was represented by a point in a specific position on the reconstructed surface shape of the model.

Since only little is known about the shape, dimensions or orientation of ribosomal proteins *in situ*, each protein was represented by a sphere with volume proportional to its molecular weight. Hydration was assumed to be 0.2 g/g. The radius (r) of each sphere was thus calculated by the relation

$$r = 0.672 * Mr^{1/3},$$

in order to obtain the best correspondence with the actual volumes of the proteins *in situ* (Richards, 1977). In the case of proteins L7/12, which are present in four copies per 50S ribosomal subunit, all four copies of these proteins were represented by a single ellipsoid, whose spatial dimensions corresponded to the dimensions of the 'L7/12-stalk' on the 50S ribosomal subunit, as seen by electron microscopy (Stöffler and Stöffler-Meilicke, 1986). The radii of the protein spheres are given in Table II.

The protein spheres were positioned in such a way that one region of each sphere was in contact with its respective epitope on the surface of the model, and the geometric centre of each sphere was placed inside the surface of the model. However, the spheres representing proteins L2 and L14 were positioned further into the model so that their nearest point to the model surface was approximately 20 Å away from the respective epitopes, thus taking into account that antibody binding to these two proteins suggests that the interface region of the 50S particle is not as flat as proposed by most three-dimensional models, but instead there is a significant concavity (Hackl *et al.*, 1988). The ellipsoid representing the four copies of proteins L7/12 was positioned in the model so that its orientation corresponded to the orientation of the 'L7/12-stalk' in the 50S subunit.

By combining the cross-linking and IEM-data five proteins not so far located by IEM, namely L3, L13, L22, L32 and L33, could be positioned in the model at clearly defined positions, since each of these proteins has been found cross-linked to two or three other proteins, whose location in the ribosome have been clearly established by IEM (Table I). The strategy for generating the three-dimensional positions for these proteins is described in detail in the following section, using protein L33 as an example: two cross-linked protein complexes containing protein L33 have been identified, namely L1−L33 and L27−L33. The spatial positions of proteins L1 and L27 (both of which have been located by IEM) were built into the model as described above, the epitope−epitope distance for proteins L1 and L27 on the surface of the IEM-model being 100 Å. Addition of the diameters of the L1, L33 and L27 protein spheres together with the length of the cross-linking reagents which gave the L1−L33 and L27−L33 crosslinks yields a value for the parameter A of 115 Å (Table I). If A (= 115 Å) and the epitope−epitope distance (= 100 Å) had been of equal value, then the geometric centre of protein L33 would have to be placed directly in line with proteins L1 and L27 at the exact mid-point of the line connecting the centres of the latter proteins. In other words, the geometric constraints in positioning a protein are the strongest, when the difference between A and the corresponding epitope−epitope distance is the least. Since in the case of protein L33 the difference between the two values is small (15 Å), the positioning of L33 is strongly constrained, and thus (within the given limits of resolution) protein L33 was placed in the space exactly between proteins L1 and L27. Equally small were the differences for the corresponding data used in placing proteins L32, L22, L13 and L3 in the model, namely 6 Å, 19 Å, 12 Å and 12 Å, respectively. Due to the strong geometric constraints imposed on the spatial position of these proteins by a network of further cross-links (see Table I) in combination with the IEM data, definitive three-dimensional positions for these proteins within the model could be determined.

For a second group of five proteins, namely L16, L21, L28, L30 and L34, the geometric constraints were not as rigorous as those for the first group just described, since each of these five proteins has been cross-linked to only one other protein localized by IEM (see Table I). Nevertheless, it was still possible to localize these proteins in distinct regions of the model. The topographical data for these proteins demanded that a point on the surface of the respective protein in the model should not be more distant

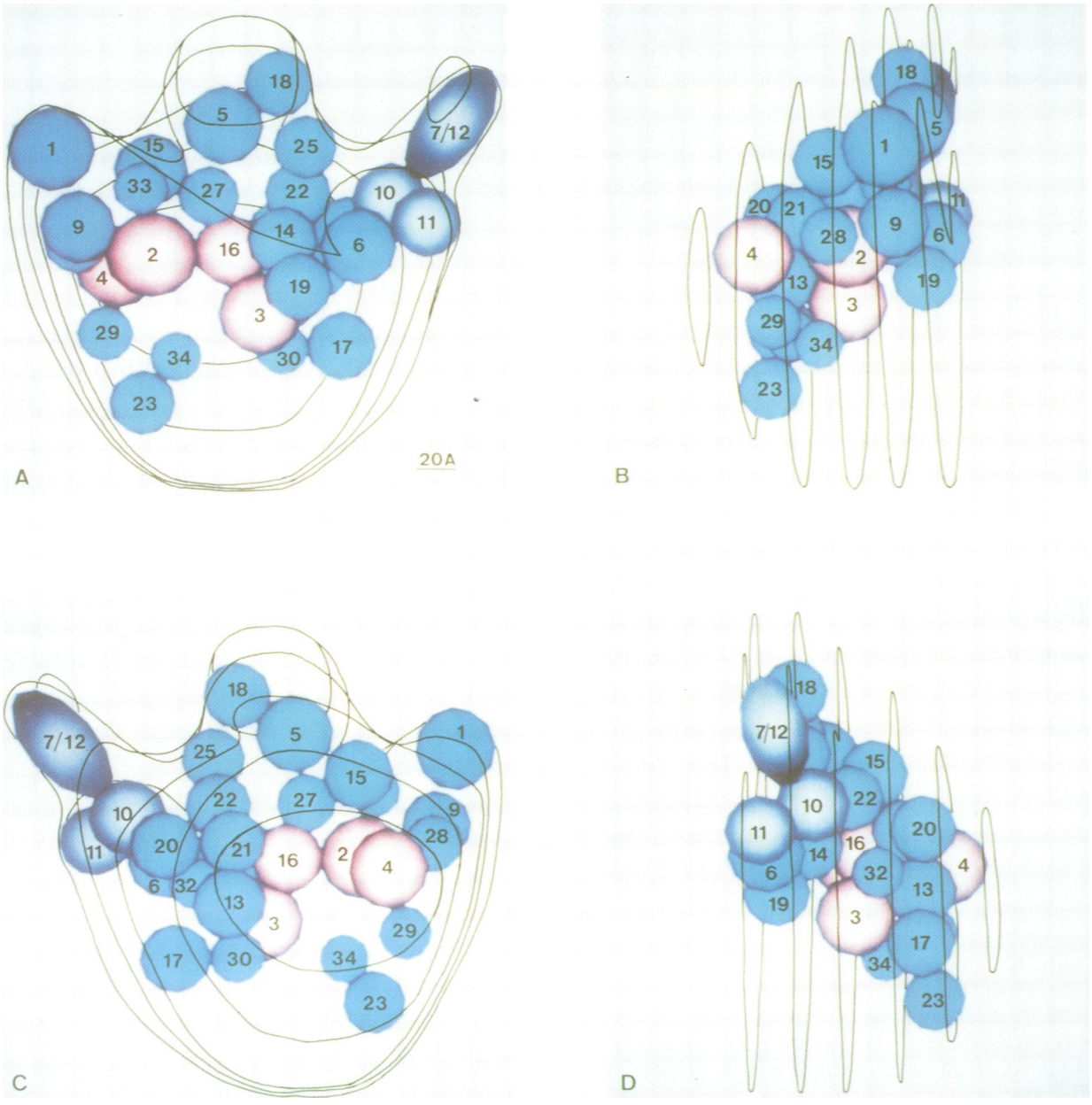

Fig. 1. Four views of the computer graphics model of the protein topography within the 50S ribosomal subunit. The individual proteins are represented as spheres with exception of the four copies of proteins L7/12 which are represented by an ellipsoid. Proteins coloured in red and blue are functionally involved in the peptidyl transferase and GTPase activity, respectively. The orientations of the four views are (**A**) 360°, (**B**) 90°, (**C**) 180°, (**D**) 270°. The views in (A) and (C) correspond to the crown views from EM; the views in (B) and (D) are slightly different from the kidney views. For details see text.

from a given protein localized by IEM than maximally 5 Å (for proteins L16, L21 and L28) or 14 Å (for proteins L30 and L34), since this is the length of the respective cross-linking reagents used to cross-link these proteins. This information allowed us to place these proteins in a clearly defined region in the model, but did not determine their locations precisely. For this reason, these proteins were positioned within the limits of the constraints so as to be as close as possible to the geometric centre of the model, taking into account steric hindrance by other proteins. By this approach locations for proteins L16, L21, L28, L30 and L34 could be established.

The Cartesian coordinates derived for the geometric centres of the individual proteins are given in Table II, and Figure 1 shows four views of the model of the 50S ribosomal subunit: (A) 'crown' projection with interface side facing the viewer, (B) 'kidney-like' projection with the L1-protuberance facing the viewer, (C) 'crown' projection with the 'back' of the subunit facing the viewer, and (D) 'kidney-like' projection with the 'L7/12-stalk' facing the viewer. At first sight, one of the most striking features of the model is that almost all of the 29 proteins so far positioned in the model are distributed fairly evenly through the upper two thirds of the model, whereas the lower third of the model,

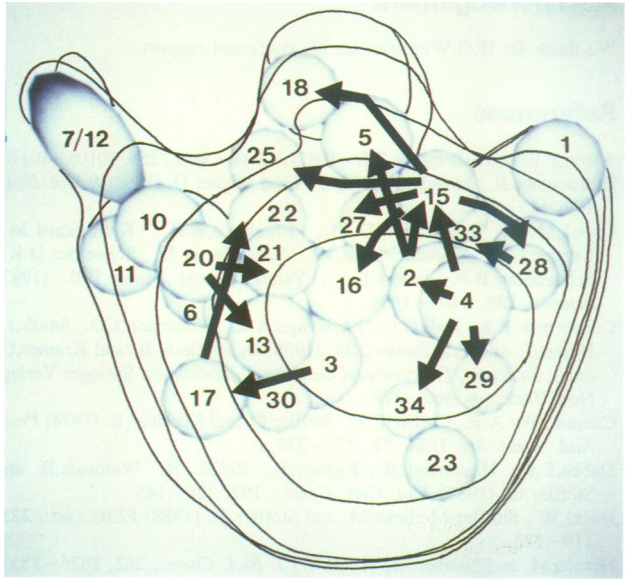

Fig. 2. Protein interactions during *in vitro* assembly of the 50S subunit. The figure shows the topographical relationships of the proteins interacting functionally in the assembly process. During the subunit assembly a protein at the head of an arrow strongly depends on the prior presence of the protein located at the tail of the arrow (Herold and Nierhaus, 1987). In this figure these relationships are shown for the proteins whose surfaces are closer than 45 Å to each other (for details see text). The view is the same as that of Figure 1C.

especially at the interface with the 30S subunit (see for example Figure 1B) in the 70S ribosome, is protein-poor.

Discussion

The model-building strategy described in this paper yields a coherent picture of the topography of the 50S subunit, and the same strategy could in principle be applied to any structure for which there are appropriate distance data available. It is important to note that for the construction of the model the degree of geometric constraint varied considerably among the different proteins. The reliability and significance of the model can therefore best be assessed by a comparison with other topographical information that was not used in its construction.

First, we discuss our model in relation to the data from protein–protein cross-linking. Until it was shown that identification of cross-linked protein pairs by diagonal gel electrophoresis can lead to misidentifications (J.Walleczek, B.Redl, M.Stöffler-Meilicke and G.Stöffler, in preparation) there was considerable disagreement among protein–protein cross-linking data for the 50S subunit. In our own cross-linking study using immunoblotting for an unambiguous identification of the individual members of the cross-links the following cross-linked protein pairs were formed by two or more different cross-linking reagents: L1–L33, L2–L9, L3–L13, L3–L19, L9–L28, L10–L11, L13–L20, L13–L21, L14–L19, L16–L27, L17–L32, L19–L25, L20–L21 and L23–L34. All these cross-links have been used as input in the model building process (Table I) and, thus, are naturally in agreement with the model. In addition, the cross-links L2–L9–L28, L5–L7/12 and L23–L29 have been identified by at least two independent groups, including ours (Traut *et al.*, 1986; J.Walleczek, T.Martin, B.Redl, M.Stöffler-Meilicke and G.Stöffler, in preparation). Whereas the cross-links L2–L9–L28 and L23–L29 are in good agreement, some assumptions have to be made for the cross-link L5–L7/12 in order to make it compatible with our model (see Figure 1a and b); either at least one of the four copies of proteins L7/12 extends towards the central protuberance, or alternatively the 'L7/12-stalk' is in itself flexible and can thus be cross-linked to protein L5 in the central protuberance, as has been suggested by several studies (for review see Möller and Maassen, 1986).

A number of ribosomal proteins that are located in proximity to the peptidyl transferase (PTF) centre have been identified in several studies, e.g. by affinity-labelling of proteins *in situ* using modified derivatives of ligands such as tRNA or antibiotics. A set of proteins has consistently been found in this type of study, namely proteins L2, L14, L15, L16, L23 and L27 (Czernilofsky *et al.*, 1974; Ofengand, 1980; Ofengand *et al.*, 1986; Cooperman *et al.*, 1986). Proteins involved in PTF activity have been identified by partial reconstitution experiments. The results showed that in addition to 23S rRNA, proteins L2, L3, L4, L15 and L16 are required to reconstitute this activity *in vitro* (Schulze and Nierhaus, 1982). The same set of proteins (with the exception of L15 which was only essential in *E.coli*) was identified in similar reconstitution experiments with ribosomal components from *Bacillus stearothermophilus* (Auron and Fahnestock, 1981). Taken together, proteins in vicinity of the PTF centre as identified by affinity-labelling and partial reconstitution form a distinct structural domain extending from the base of the central protuberance towards the L1-protuberance and the geometric centre of the model (see Figure 1). Only protein L23 is not in the immediate neighbourhood of this group of proteins in our model. Since mutants from *E.coli* lacking protein L15 (Lotti *et al.*, 1983) or protein L27 (Dabbs *et al.*, 1983) have been isolated, these two proteins should not be involved in PTF activity; we thus remain with four proteins, namely L2, L3, L4 and L16 that are involved in PTF activity and that form a distinct structural domain within the subunit (see Figure 1).

In a similar way the ribosomal proteins that are involved in translocation have been identified from a variety of studies as L6, L7/12, L10, L11 and L14, although only L7/12, L10 and L11 are known to be directly functionally involved in elongation factor G-dependent GTP hydrolysis (Möller and Maassen, 1986). Again the proteins of both these subgroups are close neighbours (see Figure 1). The model also demonstrates that the proteins involved in GTPase activity are located in a different region from those involved in PTF activity, and thus that the two major biochemical functions of the 50S ribosomal subunit during the elongation cycle in protein synthesis, namely peptide bond formation and translocation, take place in two spatially distinct regions of the subunit (Figure 1). Protein L14 may be the link between the two domains, although it should be borne in mind that the domains could partially overlap if some of the proteins concerned have elongated shapes.

Another notable correlation between structure and function comes from a comparison of our model with the assembly map for the 50S ribosomal subunit, which defines interactions between ribosomal components during the assembly process (Herold and Nierhaus, 1987). The model shows that proteins which interact during the assembly process are, with few exceptions, also spatial neighbours. For instance, protein L20 interacts directly with proteins L13, L17, L21 and L22 during subunit assembly. In addition, protein L21 stimulates

the incorporation of protein L30, and L17 stimulates the incorporation of proteins L22 and L32. Thus these proteins all interact during the assembly of the 50S ribosomal subunit, and all seven are located in a distinct domain at the 'back' of the subunit (see Figure 2). A similar group of interacting proteins is comprised of proteins L2, L4, L15, L29 and L34. Protein L4 stimulates the incorporation of proteins L2, L15, L29 and L34 directly, and all five proteins are found as neighbours, with L4 located at the centre of the group (Figure 2).

Since it could be argued that these structure–function relationships exist only for a few selected assembly dependencies, we have quantitatively analysed all the strong binding dependencies. Of the 22 strong dependencies (Herold and Nierhaus, 1987), 21 could be compared with our model. The data concerning protein L24 could not be analysed, since L24 has not yet been located in our model. The results are the following: the proteins involved in 16 out of the 21 interactions are close neighbours in the model (close neighbourhood being defined as the surfaces of the proteins lying less than 45 Å apart), and only in five cases, namely L15/L10, L15/L17, L3/L15, L4/L22, L17/L28, are the respective proteins more distant from each other (see Figure 2). This demonstrates that >75% of the strong interactions occurring during the assembly process involve proteins which later become neighbours in the mature 50S subunit. A similar correlation has been observed in the case of the 30S subunit (Moore *et al.*, 1986). Another conclusion derived from the correlation between the assembly map and our model is that those proteins in the model (L3, L4, L13, L20, L22) which form the assembly nucleus (Herold and Nierhaus, 1987) are located in a region at the 'back' of the 50S subunit, suggesting that this region functions as the starting point in the assembly process (compare Figure 1C and D).

The model presented here is clearly open to refinement, especially since four proteins, namely L24, L31, and the recently identified proteins L35 and L36 (Wada and Sako, 1987) have not yet been positioned in the model. However, the satisfying level of agreement of the model with independent structural and functional data, e.g. affinity-labelling studies, partial reconstitution experiments, and with the assembly map, suggests that the model is a good approximation of the true protein quaternary structure of the 50S ribosomal subunit. An important test of the model will obviously come from the results of neutron scattering experiments (Nowotny *et al.*, 1986) similar to those that have been made with the 30S subunit (Capel *et al.*, 1987). However, until a complete neutron data set becomes available for the 50S subunit, our model should serve as a useful framework for future investigations of ribosomal structure and function.

Materials and methods

The data used in the construction of the model are the coordinates measured from the model of the 50S ribosomal subunit as determined by IEM (Stöffler and Stöffler-Meilicke, 1986; Hackl *et al.*, 1988; W.Hackl and M.Stöffler-Meilicke, in preparation) and distances between ribosomal proteins *in situ* as determined by chemical cross-linking using specific immunoreaction in the analysis of the cross-linked proteins (Stöffler *et al.*, 1988; see Table I). The data were fed into an Evans and Sutherland PS 300 computer graphics system.

Acknowledgement

We thank Dr H.G.Wittmann for his continued support.

References

Auron,P.E. and Fahnestock,S.R. (1981) *J. Biol. Chem.*, **256**, 10105–10110.
Brimacombe,R., Atmadja,J., Stiege,W. and Schüler,D. (1988) *J. Mol. Biol.*, **199**, 115–136.
Capel,M.S., Engelmann,D.M., Freeborn,B.R., Kjeldgaard,M., Langer,J.A., Ramakrishnan,V., Schindler,D.J., Schneider,D.K., Schoenborn,B.P., Sillers,I.-Y., Yabuki,S. and Moore,P.B. (1987) *Science*, **238**, 1403–1406.
Cooperman,B.S., Hall,C.C., Kerlavage,A.R., Wetzmann,C.J., Smith,J., Hasan,T. and Friedlander,J.D. (1986) In Hardesty,B. and Kramer,G. (eds), *Structure, Function and Genetics of Ribosomes*. Springer Verlag, New York, pp. 362–378.
Czernilofsky,A.P., Collatz,E.E., Stöffler,G. and Kuechler,E. (1974) *Proc. Natl. Acad. Sci. USA*, **71**, 230–234.
Dabbs,E.R., Hasenbank,R., Kastner,B., Rak,K.-H., Wartusch,B. and Stöffler,G. (1983) *Mol. Gen. Genet.*, **192**, 129–145.
Hackl,W., Stöffler-Meilicke,M. and Stöffler,G. (1988) *FEBS Lett.*, **223**, 119–123.
Herold,M. and Nierhaus,K.H. (1987) *J. Biol. Chem.*, **262**, 8826–8833.
Lotti,M., Dabbs,E.R., Hasenbank,R., Stöffler-Meilicke,M. and Stöffler,G. (1983) *Mol. Gen. Genet.*, **192**, 295–300.
Meisenberger,O., Pilz,I., Stöffler-Meilicke,M. and Stöffler,G. (1984) *Biochim. Biophys. Acta*, **781**, 225–233.
Möller,W. and Maassen,J.A. (1986) In Hardesty,B. and Kramer,G. (eds), *Structure, Function and Genetics of Ribosomes*. Springer Verlag, New York, pp. 309–325.
Moore,P.B., Capel,M., Kjeldgaard,M. and Engelman,D.M. (1986) In Hardesty,B. and Kramer,G. (eds), *Structure, Function and Genetics of Ribosomes*. Springer Verlag, New York, pp. 87–100.
Nowotny,V., May,R.P. and Nierhaus,K.H. (1986) In Hardesty,B. and Kramer,G. (eds), *Structure, Function and Genetics of Ribosomes*. Springer Verlag, New York, pp. 101–111.
Ofengand,J. (1980) In Chambliss,G., Craven,G.R., Davies,J., Davis,K., Kahan,L. and Nomura,M. (eds), *Ribosomes: Structure, Function and Genetics*. University Park Press, Baltimore, pp. 497–530.
Ofengand,J., Ciesiolka,J., Denman,R. and Nurse,K. (1986) In Hardesty,B. and Kramer,G. (eds), *Structure, Function and Genetics of Ribosomes*. Springer Verlag, New York, pp. 473–494.
Radermacher,M., Wagenknecht,T., Verschoor,A. and Frank,J. (1987) *EMBO J.*, **6**, 1107–1114.
Richards,F.M. (1977) *Annu. Rev. Biophys. Bioeng.*, **6**, 151–176.
Schüler,D. and Brimacombe,R. (1988) *EMBO J.*, **7**, 1509–1513.
Schulze,H. and Nierhaus,K.H. (1982) *EMBO J.*, **1**, 609–613.
Stöffler,G., Redl,B., Walleczek,J. and Stöffler-Meilicke,M. (1988) *Methods Enzymol.*, **164**, 64–76.
Stöffler,G. and Stöffler-Meilicke,M. (1985) *Annu. Rev. Biophys. Bioeng.*, **13**, 303–330.
Stöffler,G. and Stöffler-Meilicke,M. (1986) In Hardesty,B. and Kramer,G. (eds), *Structure, Function and Genetics of Ribosomes*. Springer Verlag, New York, pp. 28–46.
Stöffler-Meilicke,M. and Stöffler,G. (1987) *Biochimie*, **69**, 1049–1064.
Traut,R.R., Tewari,D.S., Sommer,A., Gavino,G.R., Olson,H.M. and Glitz,D.G. (1986) In Hardesty,B. and Kramer,G. (eds), *Structure, Function and Genetics of Ribosomes*. Springer Verlag, New York, pp. 286–308.
Wada,A. and Sako,T. (1987) *J. Biochem.*, **101**, 817–820.

Received on July 5, 1988; revised on September 2, 1988